ACS OMEGA

Article

Cite This: ACS Omega 2019, 4, 9860−9867

http://pubs.acs.org/journal/acsodf

Synthesis and Functionalization of Porous Zr-Diaminostilbenedicarboxylate Metal−Organic Framework for Storage and Stable Delivery of Ibuprofen

Mithun Sarker, Subin Shin, and Sung Hwa Jhung*

Department of Chemistry and Green-Nano Materials Research Center, Kyungpook National University, Daegu 41566, Republic of Korea

Supporting Information

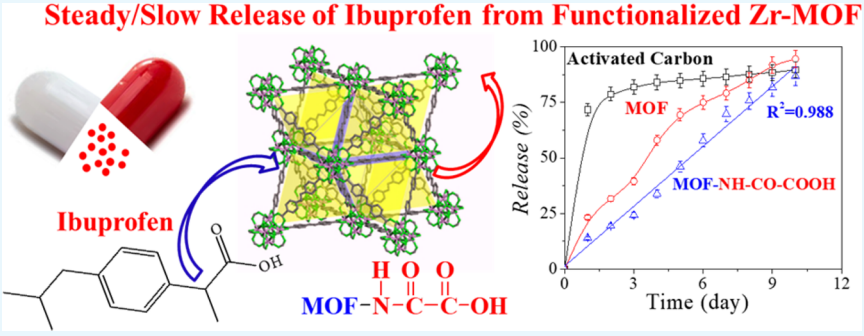

ABSTRACT: A stable porous metal−organic framework (MOF), Zr-diaminostilbenedicarboxylate (Zr-DASDCA), was synthesized and modified with oxalyl chloride (OC) or terephthaloyl chloride (TC) to introduce various functional groups onto the Zr-DASDCA. Both pristine and functionalized Zr-DASDCAs, together with activated carbon, were used as a potential carrier for ibuprofen (IBU) storage and delivery. Zr-DASDCAs, especially the modified ones (OC-Zr-DASDCA and TC-Zr-DASDCA), showed competitive results in IBU delivery. Specifically, the release rate in phosphate-buffered saline solution at pH 7.4 was nearly constant ($R^2 \approx 0.98$) for up to 10 days, which would be very effective in IBU dosing to the human body. Moreover, the release rate could be controlled by changing the pH of the releasing solution. The rate of IBU release from both pristine and modified Zr-DASDCAs at pH 7.4 and 3.0 was also explained with a few interactions such as H-bonding and electrostatic repulsion, together with the relative pore size of the Zr-DASDCAs. Therefore, the results suggested that functionalization of MOFs via postsynthetic modification, especially with OC and TC, to introduce various functional groups onto MOFs is an effective approach to not only reducing the release rate of IBU but also inducing a constant release of IBU for as long as 10 days.

1. INTRODUCTION

Metal−organic frameworks (MOFs)[1−4] are an advanced class of fascinating porous materials that have attracted the attention of researchers because of their simple synthesis, exclusive characteristics, facile modification, and potential applications.[5−9] Various approaches,[10,11] including functionalization, have been widely used in the past decades to enhance the performance of MOFs.[12−14] Postsynthetic modification (PSM) is considered to be one of the most attractive strategies to introduce additional functional groups onto MOFs because it involves simple and effective processes.[15,16] MOFs with amino groups have been reported to be easily modified to introduce different functionalities via covalent PSM.[17−19] For example, amino-MOFs were modified covalently with various reagents such as aldehydes,[20] acetic anhydride,[21] phenyl isocyanate,[22] polyethyleneimine,[23] and peptide coupling reagents.[24] However, the covalent PSM of many microporous MOFs might be hindered by their low stability and small pore size.

Among MOFs, zirconium-MOFs (Zr-MOFs) usually possess excellent chemical, thermal, and water stability because of strong Zr−O bonds and a stable secondary building unit.[25,26] For example, an amino-functionalized Zr-MOF, Zr-diaminostilbenedicarboxylate (Zr-DASDCA, also known as JLU-Liu36 or UBMOF-8 and composed of robust $Zr_6O_4(OH)_4$ clusters), is stable and contains large pores,[27,28] rendering it suitable for PSM. Moreover, functionalized Zr-MOFs are very attractive because of their potential applications, especially in biomedical fields and drug delivery.[29,30] Therefore, the possible functionalization of Zr-MOFs, especially NH_2-functionalized Zr-MOFs, through covalent modification might be interesting and warrants further research because it potentially represents a simple process to introduce additional functionalities onto MOFs.

Received: April 19, 2019
Accepted: May 24, 2019
Published: June 5, 2019

DOI: 10.1021/acsomega.9b01139
ACS Omega 2019, 4, 9860−9867

Ibuprofen (IBU, 4-isobutyl-α-methylphenylacetic acid) is one of the most consumed nonsteroidal anti-inflammatory drugs in the world.[31] IBU is a well-defined drug with a molecular size of ~1.03 × 0.53 nm and is commonly used as a model drug for delivery.[31] The typical therapeutic range and toxic level of IBU in human blood are approximately 10−50 mg·L^{-1} and greater than 250 mg·L^{-1}, respectively.[31,32] An overdose of IBU adversely affects the nervous system, respiratory tract, and gastrointestinal tract and leads to renal failure.[31] Therefore, controlled release of IBU from a suitable IBU-loaded carrier is required. Several porous materials such as mesoporous and nanoporous silica,[33] polymeric materials,[34,35] titania nanotubes,[36] mesoporous carbon,[31] bionanocomposites,[37] and MOFs[38−43] are commonly applied for IBU delivery. Among these materials, MOFs are attractive because they enable a high loading of IBU (because of feature-specific interactions between the drug and carrier[9,44]), even though polymeric carriers[45,46] showed very high loading (~80%) for some anticancer drugs. Moreover, in the case of controlled drug delivery, the pore size and functionality of carriers strongly affect cellular uptake and subsequent delivery or transportation of a drug into the human body.[47] Therefore, delivery of IBU from functionalized MOFs, especially Zr-MOFs, might be interesting and should be researched further, given the possibilities of adequate loadings and controlled release.

Herein, we report a postsynthetic modification of a NH_2-Zr-MOF (Zr-DASDCA) with oxalyl chloride (OC) and terephthaloyl chloride (TC) to introduce carboxylic, phenyl, and amide functional groups onto MOFs. Because of the low toxicity of Zr and carboxylic acids, the functionalized MOFs (named OC-Zr-DASDCA and TC-Zr-DASDCA, respectively) were used to store/deliver IBU.[9,48] Zr-DASDCAs in both pristine and modified forms showed a much higher IBU loading and slower release of IBU compared with commercial activated carbon (AC). Importantly, OC-Zr-DASDCA and TC-Zr-DASDCA exhibited nearly constant release (with slow rate) of IBU in 10 days, unlike pristine Zr-DASDCA and AC. Moreover, the release rate of IBU from modified Zr-DASDCAs could be controlled by changing the pH of the solution for delivery.

Table 1. Textural Properties of AC and MOFs Used in This Study

material	BET surface area ($m^2 \cdot g^{-1}$)	total pore volume ($cm^3 \cdot g^{-1}$)	micropore volume ($cm^3 \cdot g^{-1}$)
AC	1016	0.56	0.29
Zr-DASDCA	1889	0.86	0.58
OC-Zr-DASDCA	1622	0.70	0.48
TC-Zr-DASDCA	1437	0.62	0.40

2. RESULTS AND DISCUSSION

2.1. Characterization of Carriers. The XRD patterns of Zr-DASDCA with and without modification are shown in Figure 1a. The XRD patterns of the pristine and modified MOFs are in agreement with the simulated pattern for Zr-DASDCA, certifying not only the successful synthesis of pristine Zr-DASDCA but also the structural integrity of the Zr-DASDCA during modifications. The presence of different functional groups on the MOFs was confirmed by the FTIR

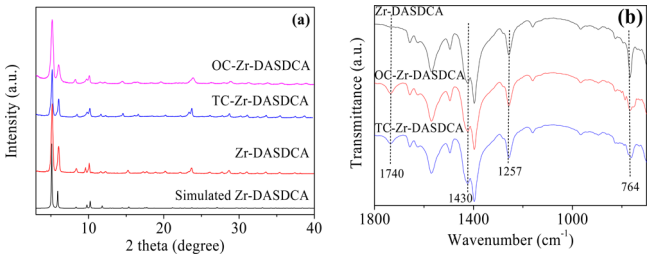

Figure 1. (a) XRD patterns and (b) FTIR spectra of Zr-DASDCAs. The simulated XRD pattern of Zr-DASDCA is also shown in (a) for comparison.

spectra (Figure 1b). The pristine and modified Zr-DASDCAs showed absorption bands at 1257 and 1430 cm^{-1}, which were assigned as the C−N stretching vibrations of the MOFs.[27,49,50] The spectrum of the pristine Zr-DASDCA also showed a N−H wagging band at ~764 cm^{-1}; this band was less intense in the case of OC-Zr-DASDCA and TC-Zr-DASDCA because of the introduction of additional functionalities on the $-NH_2$ group via PSM,[50,51] as shown in Scheme 1 for OC-Zr-DASDCA.

Scheme 1. Scheme for the Synthesis of Zr-DASDCA and OC-Zr-DASDCA

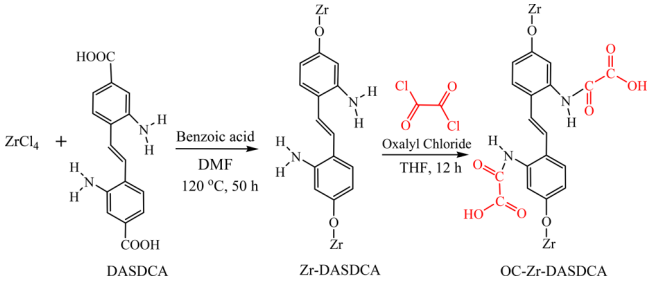

Moreover, the existence of a broad band at ~1740 cm^{-1} affirms the presence of free −COOH groups[50,52] in both OC-Zr-DASDCA and TC-Zr-DASDCA as a result of the modification. Additionally, the degree of modification of the MOFs was calculated on the basis of the total quantity of −COOH groups present in the studied MOFs, which were measured by acid−base titration. As shown in Table 2, the total amount of

Table 2. Concentrations of −COOH Groups Determined by Acid−Base Titration and Yields of Modification of Zr-DASDCA

MOF	experimental concentration of −COOH groups ($mmol \cdot g^{-1}$)	stoichiometric concentration of −COOH groups ($mmol \cdot g^{-1}$)	degree of modification of MOFs (%)
Zr-DASDCA	0.17	0.0	
OC-Zr-DASDCA	1.36	2.07	56%
TC-Zr-DASDCA	0.94	1.79	43%

−COOH groups in OC-Zr-DASDCA or TC-Zr-DASDCA was much higher than that in pristine Zr-DASDCA because of the modifications. The degrees of functionalization in OC-Zr-DASDCA and TC-Zr-DASDCA were 56 and 43%, respectively.

The nitrogen adsorption isotherms and pore size distributions of the Zr-DASDCAs are shown in Figure 2a,b, respectively. The BET surface areas and pore volumes of the studied materials, as calculated from the N_2 isotherms, are

DOI: 10.1021/acsomega.9b01139
ACS Omega 2019, 4, 9860−9867

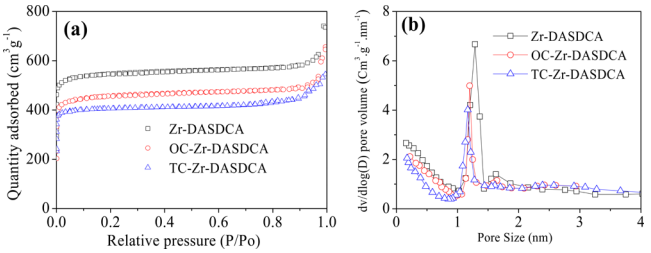

Figure 2. (a) Nitrogen adsorption−desorption isotherms and (b) pore size distributions of Zr-DASDCAs.

summarized in Table 1. The porosity of modified Zr-DASDCAs was reduced after functionalization of the pristine Zr-DASDCA because of the attachment of additional functional groups onto the MOF surface.[53] The pore size of the pristine MOF was ∼1.3 nm, consistent with the previously reported result;[27] however, the pore size of the Zr-DASDCA decreased after modification and exhibited the order pristine Zr-DASDCA > OC-Zr-DASDCA > TC-Zr-DASDCA. The order of these pore sizes can be explained on the basis of the size of extra functional groups on the modified Zr-DASDCAs. Moreover, the morphology of the Zr-DASDCAs together with AC was studied by using electron microscopy. The SEM images presented in Figure S2 were similar to earlier reports[27,28] and showed that the morphology of modified Zr-DASDCAs did not change during modification with OC and TC.

2.2. Adsorption of IBU. The prepared MOFs or commercial AC was employed separately for IBU loading through adsorption. The loaded quantities of IBU over the studied materials were examined for a contact period of 6 to 24 h (q_{6h}−q_{24h}). The performances of the studied materials for IBU adsorption are shown in Figure 3. Interestingly, OC-Zr-

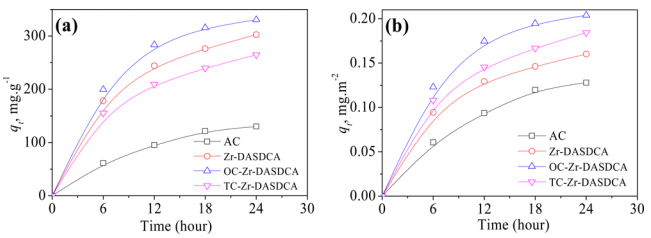

Figure 3. Effect of contact time (a) based on unit weight and (b) based on surface area on IBU adsorptions over AC and Zr-DASDCAs. The initial concentration of IBU was 5000 mg·L^{-1} in ethanol.

DASDCA adsorbed a greater amount of IBU than pristine Zr-DASDCA, even though OC-Zr-DASDCA possessed a lower surface area than the pristine sample. The adsorption isotherms obtained from a wide range of initial IBU concentrations (2000−5000 mg·L^{-1}) over the studied materials and Langmuir plots[54] for IBU isotherms are shown in Figure S3. Langmuir parameters[54] such as the maximum adsorption capacities (Q_0), b-values, and correlation coefficients (R^2) are presented in Table 3. The OC-Zr-DASDCA, Zr-DASDCA, TC-Zr-DASDCA, and AC showed Q_0 values of 455, 434, 370, and 185 mg·g^{-1}, respectively. The results for b-values are also agreeable with the tendency of the Q_0 values. Alternatively, the IBU adsorption was the most favorable over the OC-Zr-DASDCA among the tested adsorbents.

Table 3. Langmuir Parameters and Loading Quantities of IBU over AC and Zr-DASDCAs for Adsorption of IBU from Ethanol

	Langmuir parameters			
material	Q_0 (mg·g^{-1})	b (L·mg^{-1})	R^2	IBU loading[a] (wt %)
AC	185	5.2 × 10^{-4}	0.996	11%
Zr-DASDCA	434	6.0 × 10^{-4}	0.998	23%
OC-Zr-DASDCA	455	7.4 × 10^{-4}	0.998	25%
TC-Zr-DASDCA	370	5.4 × 10^{-4}	0.999	21%

[a]Calculated values from q_{24h} in Figure 3 on the basis of the following equation: IBU loading = [(weight of IBU in MOF)/(weight of IBU + MOF)] × 100%

The successful loading of IBU on OC-Zr-DASDCA was confirmed by the FTIR analysis, as shown in Figure 4a. Several

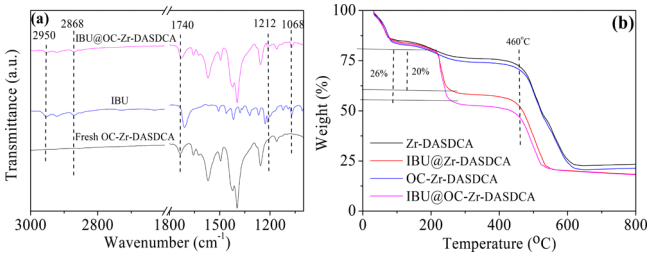

Figure 4. (a) FTIR spectra of IBU and OC-Zr-DASDCA before and after loading of IBU and (b) TGA results for Zr-DASDCA and OC-Zr-DASDCA before and after loading of IBU.

characteristic bands of IBU were detected in the spectrum of IBU@OC-Zr-DASDCA, ensuring the successful loading of IBU on the OC-Zr-DASDCA. The crystalline structure of the studied MOFs was preserved well after the encapsulation of IBU, as shown in Figure S4a, certifying the structural integrity of the studied MOFs during and after loading of the IBU. Moreover, the BET surface areas and pore volumes of IBU-loaded MOFs were determined from nitrogen adsorption isotherms; the results are shown in Figure S4b. The results, as summarized in Table S1, disclose that the porosities of the MOFs severely decreased after IBU loading, also indicating the successful encapsulation of IBU onto the MOFs' cavities. Similar results have been reported for the loading of IBU onto mesoporous carbon[31] and an MOF.[38]

The amounts of IBU loaded onto the MOFs were determined by TGA. From the TGA patterns shown in Figure 4b, three weight losses were identified at temperatures of ∼100, 200−260, and 450−600 °C. The first weight loss is attributed to the removal of physisorbed ethanol/water. The second weight loss might be volatilization of the loaded IBU (boiling point, 157 °C). The last one is attributed to destruction of the MOFs.[38,41] On the basis of the TGA results, the loaded amounts of IBU on pristine Zr-DASDCA and OC-Zr-DASDCA were ∼20 and 26%, respectively (Figure 3); these results are consistent with the values calculated using the quantities obtained from adsorption for 24 h and reported in Table 3.[55] Moreover, the loading capacities (wt %) of Zr-DASDCAs were very similar to those reported for other MOFs, as summarized in Table S2, excluding the Cr-containing MOFs (especially highly porous MIL-101(Cr)), which might be not suitable for the human body given the toxicity of chromium.[9]

DOI: 10.1021/acsomega.9b01139
ACS Omega 2019, 4, 9860−9867

The adsorption of various organics, including drug and biomolecules, has previously been explained with various adsorption mechanisms.[56−60] The amount of any adsorbate adsorbed onto a porous adsorbent usually depends on the surface area of the adsorbent in the absence of a special interaction, excluding van der Waals interaction.[61] The obtained results show that the OC-Zr-DASDCA has a higher q_{24h} for IBU adsorption than the pristine Zr-DASDCA by 9%, even though OC-Zr-DASDCA possesses a lower surface area (14% less) than pristine Zr-DASDCA. Therefore, simple van der Waals interaction, which is mainly dependent on the surface area of the adsorbent, might not be the sole mechanism by which IBU adsorbs onto OC-Zr-DASDCA. The decreased pore size of OC-Zr-DASDCA compared with that of pristine Zr-DASDCA might render it more suitable for IBU adsorption. Tailoring of the pore size (with tetraethyl orthosilicate-modified MIL-125-NH_2) has been demonstrated to be highly effective for drug delivery, especially in the case of IBU release.[40] Moreover, on the basis of the surface area, TC-Zr-DASDCA also showed increased adsorption or loading of IBU compared with pristine Zr-DASDCA (Figure 3b). The competitive loading of IBU onto TC-Zr-DASDCA might also be explained by reduced pore size. Even though an explanation of why the TC-Zr-DASDCA adsorbed less IBU (based on the surface area) than OC-Zr-DASDCA is not straightforward, the presence of a bulky phenyl ring (that might hinder the adsorption of IBU) onto TC-Zr-DASDCA and further reduction of the pore size (Figure 2b) might be some of the reasons.

2.3. Release of IBU from Loaded Carriers. The release of IBU from IBU-loaded AC or MOFs was examined using a PBS buffer solution (0.01 M at pH 7.4) for up to 10 days, as shown in Figure 5. The rapid release of IBU (~70% of loaded

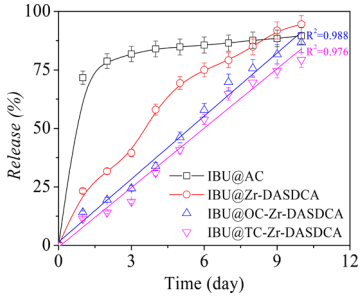

Figure 5. IBU release profiles from IBU-loaded AC and Zr-DASDCAs in PBS buffer (0.01 M) solution at pH 7.4.

IBU in 1 day) from IBU@AC was observed, similar to the results with mesoporous carbon.[31] This kind of rapid or burst release of drug molecules has been considered pharmacologically harmful and economically inefficient.[62−64] The rapid release of IBU from AC within a short time confirms that the loading of IBU on AC is mainly dependent on physical interaction or van der Waals interaction.[65] This result is easily explained by the fact that AC has a lower concentration of functional groups than Zr-DASDCAs. Moreover, the relatively large pore size of AC[66] might be one of the reasons for rapid release or diffusion. In contrast, as shown in Figure 5, the release rates of IBU from Zr-DASDCAs are relatively low (especially from modified MOFs), suggesting that the interaction between IBU and Zr-DASDCAs involves not only physisorption but also chemisorption. Approximately one-half of the loaded IBU was released in ~3.0, 5.5, and 6.0 days from pristine Zr-DASDCA, OC-Zr-DASDCA, and TC-Zr-DASDCA, respectively, suggesting a slight difference in interaction between IBU and the Zr-DASDCAs.

Importantly, compared with pristine Zr-DASDCA, the OC-Zr-DASDCA and TC-Zr-DASDCA exhibit slower and controlled release (or nearly constant release) of IBU, which is very significant for effective drug delivery.[38,67] The correlation coefficient (R^2) values for IBU delivery from IBU@Zr-DASDCA, IBU@OC-Zr-DASDCA, and IBU@TC-Zr-DASDCA are 0.914, 0.988, and 0.976, respectively, confirming that OC-Zr-DASDCA and TC-Zr-DASDCA exhibited nearly constant release for as long as 10 days. The controlled release of IBU from OC-Zr-DASDCA and TC-Zr-DASDCA might be explained by the reduced pore size and specific chemical interactions (see below).

To understand the specific interaction and controlled release of IBU from pristine and modified MOFs in the human body, the effects of pH on IBU release from IBU-loaded Zr-DASDCAs were studied. As shown in Figure 6, the delivery or

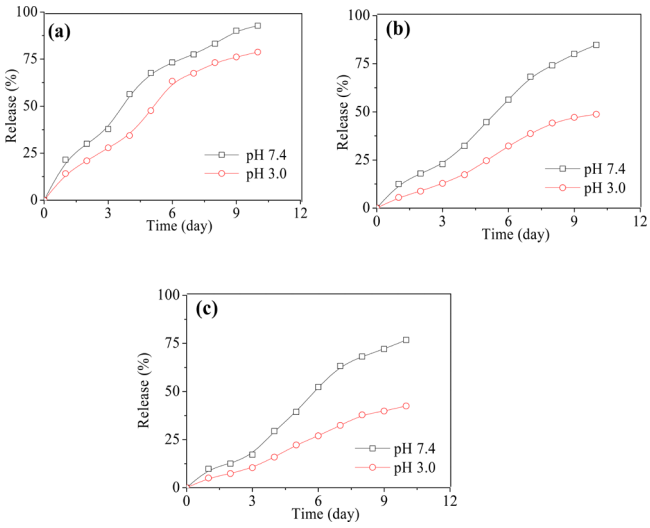

Figure 6. Effect of pH on the IBU release rate from IBU-loaded (a) Zr-DASDCA, (b) OC-Zr-DASDCA, and (c) TC-Zr-DASDCA.

release rate of IBU from IBU@OC-Zr-DASDCA or IBU@TC-Zr-DASDCA decreased considerably with decreasing solution pH (from pH 7.4 to 3.0). This result differs from that for IBU@Zr-DASDCA, which showed only a slightly decreased delivery rate at pH 3.0 compared with that at pH 7.4.

The fast release of IBU from pristine Zr-DASDCA (compared with modified Zr-DASDCAs), as shown in Figure 6, at the two pH conditions (especially at pH 3.0), might be primarily because of the relatively large pore size. On the contrary, the decreased IBU release rates from OC-Zr-DASDCA and TC-Zr-DASDCA at pH 3.0 (Figure 6b,c) might be due to small pores and favorable interaction (via H-bonding, which has been often observed in adsorption over MOFs[56,57]) between IBU and OC-Zr-DASDCA or TC-Zr-DASDCA, as shown in Scheme 2 (left, for OC-Zr-DASDCA). The IBU release rate has already been reported to decrease with decreasing pore size[40] and decreasing pH.[68] At a high pH value of 7.4, there might be a repulsive interaction (rather than H-bonding) between carboxylate anions because of facile deprotonation of both −COOH groups of IBU and OC-Zr-

DOI: 10.1021/acsomega.9b01139
ACS Omega 2019, 4, 9860−9867

Scheme 2. Plausible Interactions To Explain the Release of IBU from OC-Zr-DASDCA at pH 3.0 (left) and 7.4 (right)

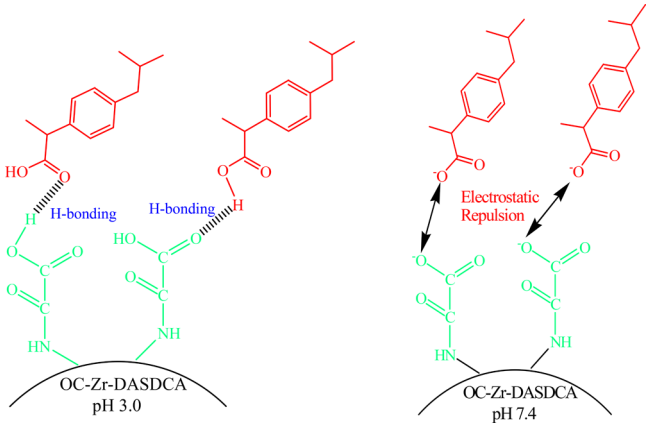

DASDCA or TC-Zr-DASDCA (since the pK_a value of the −COOH group is ∼4.9[69]). Even though H-bonding between $-COO^-$ of IBU and −NH− of OC-Zr-DASDCA or TC-Zr-DASDCA can be expected, such interaction might not be easy given the position of −NH−, whose interaction with IBU is sterically hindered. The observed release rates of loaded IBU from OC-Zr-DASDCA or TC-Zr-DASDCA at pH 7.4 (which is similar to the rates from pristine Zr-DASDCA at the two pH conditions) might be because of a tradeoff between small pores (which can decrease the release rate) and repulsive interactions (which can increase the release rate). The possible interactions of IBU with pristine Zr-DASDCA and OC-Zr-DASDCA at pH 3.0 and 7.4 are shown in Scheme S2 and Scheme 2, respectively. Finally, the possible destruction of Zr-DASDCA (especially at pH 7.4) after several days in PBS solution cannot be ruled out since, recently, it has been reported that Zr-MOFs such as UiO-66 are not very stable even in the condition of pH 7.[70] Further work is required to understand the possible contribution of destruction of Zr-DASDCAs in the delivery of IBU.

Therefore, modified Zr-DASDCAs can be suggested as effective carriers for IBU on the basis of (i) a nearly constant delivery rate for as long as 10 days, (ii) possible control of the delivery rate by changing the pH of solution, and (iii) competitive storage capacity of IBU.

3. CONCLUSIONS

On the basis of postsynthetic modification of Zr-DASDCA and the adsorption/delivery of IBU with Zr-DASDCAs, the following conclusions were obtained. First, the Zr-DASDCA could be facilely modified with OC or TC to introduce various functional groups because of large pores and the stability of the MOF. Second, modified Zr-DASDCAs (OC-Zr-DASDCA and TC-Zr-DASDCA) might be useful as carriers for IBU, as demonstrated by the very stable/constant release of IBU in PBS for as long as 10 days and possible control of the release rate by changing the pH. Third, the release rates from Zr-DASDCAs could be explained by the pore size of the MOFs, H-bonding, and electrostatic interactions. Finally, modification of MOFs such as stable/porous Zr-DASDCA with OC and TC can be suggested as an effective method for the controlled release of some drugs with carboxylic groups with slow/stable dosing for 10 days.

4. EXPERIMENTAL SECTION

4.1. Chemicals. Zirconium(IV) chloride ($ZrCl_4$, 99.5%), IBU ($C_{13}H_{18}O_2$, 99%), 4-(chloromethyl)benzoic acid ($C_8H_7ClO_2$, 96%), and benzoic acid ($C_7H_6O_2$, 99%) were purchased from Alfa Aesar. Phosphate-buffered saline (PBS, 0.01 M) and sodium sulfide anhydrous (Na_2S) were procured from Sigma-Aldrich. Oxalyl chloride ($C_2Cl_2O_2$, 98%) and terephthaloyl chloride ($C_8H_4Cl_2O_2$, 98%) were acquired from TCI Co., Ltd. Granular AC (2−3 mm, practical grade) and potassium hydroxide (KOH, 85%) were acquired from Duksan Pure Chemical Co., Ltd. and Samchun Pure Chemical Co., Ltd., respectively. Ethanol (C_2H_6O, 99%), hydrochloric acid (HCl, 37%), methanol (CH_4O, 99%), *N*,*N*-dimethylformamide (DMF, 99%), nitric acid (HNO_3, 60%), sodium hydroxide (NaOH, 98%), sulfuric acid (H_2SO_4, 95%), tetrahydrofuran (THF, 99%), and triethylamine (TEA, 98%) were obtained from OCI Co., Ltd. All of the chemicals were used without further purification.

4.2. Synthesis and Modification of MOFs. Prior to the synthesis of Zr-DASDCA, a DASDCA (2,2′-diamino-4,4′-stilbenedicarboxylic acid) linker was synthesized according to a reported procedure.[27] The detailed DASDCA linker synthesis is described in Scheme S1 in the Supporting Information. Zr-DASDCA was synthesized via the reaction between $ZrCl_4$ and DASDCA, conducted according to a previously reported procedure.[27] Briefly, 0.07 g of $ZrCl_4$, 0.10 g of DASDCA linker, and 1.8 g of benzoic acid were dissolved in 20 mL of DMF in a scintillation vial under ultrasonication. The vial was then sealed and heated for 50 h at 120 °C to produce pale orange crystals. The crystals were filtered and washed with DMF and methanol and then further dried under vacuum. The modification of pristine Zr-DASDCA was carried out using oxalyl chloride and terephthaloyl chloride according to previously described methods[49,50] to synthesize OC-Zr-DASDCA and TC-Zr-DASDCA, respectively. Oxalyl chloride (0.15 g) or terephthaloyl chloride (0.25 g) was added separately to a THF (10 mL) solution containing pristine Zr-DASDCA (0.20 g) for the synthesis of OC-Zr-DASDCA and TC-Zr-DASDCA, respectively. After 2 h, TEA (0.12 g) was added dropwise to the mixture, which was then further stirred for 12 h at room temperature. The preparation and modification (for the case of oxalyl chloride) of Zr-DASDCA are illustrated in Scheme 1.

4.3. Characterization of MOFs. The crystal structures of the pristine and modified Zr-DASDCAs were analyzed using an X-ray diffractometer (Bruker, D2 Phaser) equipped with a Cu Kα radiation source. The textural properties of the prepared MOFs were determined by nitrogen adsorption at −196 °C with a porosity analyzer (TriStar II 3020, Micromeritics) after evacuation of the MOFs overnight at 120 °C. The surface areas of the prepared MOFs were calculated with the Brunauer−Emmett−Teller (BET) equation. The pore size of the studied MOFs was calculated by applying Barrett−Joyner−Halenda (BJH) equation to the desorption branch of nitrogen adsorption isotherms. Fourier-transform infrared spectroscopy (FTIR) was conducted with an instrument (Jasco FTIR-4100) fitted with an attenuated total reflectance (ATR) module (maximum resolution: 4.0 cm^{-1}). The results confirmed not only the successful modification of Zr-DASDCA but also the loading of IBU onto OC-Zr-DASDCA. Thermogravimetric analysis (TGA) was carried out using a PerkinElmer TGA 4000 system under nitrogen flow from 30 to 800 °C at a heating rate of 10 °C

DOI: 10.1021/acsomega.9b01139
ACS Omega 2019, 4, 9860−9867

min^{-1} to determine the amount of IBU loaded onto the MOFs. In addition, the successful synthesis of the DASDCA linker was confirmed from the ^1H NMR spectrum obtained using an NMR spectrometer (Bruker, AVANCE III 500, 500 MHz), as shown in Figure S1. Moreover, the acid−base titration method was utilized to determine the free −COOH concentrations in the modified Zr-DASDCAs.

4.4. Adsorption of IBU onto Zr-DASDCAs and AC. Zr-DASDCAs or commercial AC (50 mg each) was immersed in 20 mL of IBU solution (concentration: 5000 $mg{\cdot}L^{-1}$ in ethanol), and the mixture was stirred at 200 RPM using an incubated shaker for 6−24 h at 25 °C. After adequate intervals (6, 12, 18, and 24 h), the mixture was separated using a nylon membrane filter. After 24 h of adsorption, IBU-loaded solids were recovered by filtration and further washing three times with ethanol and then finally with water. The recovered solids, after 24 h of adsorption, were used in a delivery study (see below). The remaining concentrations of IBU in liquid solution, after each adsorption, were assessed by measuring the absorbance of the solution at 220 nm using a UV spectrometer (UV-1800, Shimadzu).[69] Adsorption isotherms were obtained similarly after adsorption for 24 h using solutions with different IBU concentrations (2000−5000 $mg{\cdot}L^{-1}$); the adsorption results were calculated using Langmuir isotherm.[54]

4.5. Release of IBU from Zr-DASDCAs and AC. Four batches of the filtered MOFs or AC (obtained after adsorption for 24 h and separation) were mixed well with a spatula, dried overnight at room temperature, and used in the delivery or release study. Moreover, the structural integrity and textural parameters of the dried IBU-loaded Zr-DASDCAs were checked by XRD analysis and nitrogen adsorption experiments, respectively, to confirm the stability of the loaded MOFs and the successful IBU uptake. The release of IBU from pristine and modified Zr-DASDCAs and AC was performed in PBS solution. Typically, 10 mg of dried IBU-loaded materials was dispersed into 10 mL of PBS solution (pH 7.4, concentration of 0.01 M) at 37 °C, and the mixture was shaken for 1−10 days, similar to the procedure used in the adsorption study. After completion of the release experiments in the desired time, the PBS solutions were filtered using a polytetrafluoroethylene syringe filter (hydrophobic, 0.5 μm), and the concentration of released IBU in the solution was examined similarly by UV spectrometry. The effect of pH on the release of IBU from pristine and modified Zr-DASDCAs was also studied by checking the release rates at pH 3.0, together with those at pH 7.4.

■ ASSOCIATED CONTENT

Supporting Information

The Supporting Information is available free of charge on the ACS Publications website at DOI: 10.1021/acsomega.9b01139.

Materials, characterization results, adsorption, and release data (PDF)

■ AUTHOR INFORMATION

Corresponding Author

*E-mail: sung@knu.ac.kr. Phone: 82-53-950-5341. Fax: 82-53-950-6330.

ORCID

Sung Hwa Jhung: 0000-0002-6941-1583

Author Contributions

The manuscript was written through contributions of all authors. All authors have given approval to the final version of the manuscript.

Funding

This work was supported by the National Research Foundation of Korea (NRF) grant funded by the Korea Government (MSIP) (grant number 2017R1A2B2008774).

Notes

The authors declare no competing financial interest.

■ ABBREVIATIONS

AC, activated carbon; BET, Brunauer−Emmett−Teller; BJH, Barrett−Joyner−Halenda; DASDCA, diaminostilbenedicarboxylate; FTIR, Fourier-transform infrared spectrometer; H-bonding, hydrogen-bonding; IBU, ibuprofen; OC, oxalyl chloride; PBS, phosphate-buffered saline; PSM, postsynthetic modification; TC, terephthaloyl chloride

■ REFERENCES

(1) Wang, C.; Liu, X.; Demir, N. K.; Chen, J. P.; Li, K. Applications of Water Stable Metal-Organic Frameworks. *Chem. Soc. Rev.* **2016**, *45*, 5107−5134.

(2) Cui, Y.; Li, B.; He, H.; Zhou, W.; Chen, B.; Qian, G. Metal−Organic Frameworks as Platforms for Functional Materials. *Acc. Chem. Res.* **2016**, *49*, 483−493.

(3) Kirchon, A.; Feng, L.; Drake, H. F.; Joseph, E. A.; Zhou, H.-C. From Fundamentals to Applications : A Toolbox for Robust and Multifunctional MOF Materials. *Chem. Soc. Rev.* **2018**, *47*, 8611−8638.

(4) Howarth, A. J.; Peters, A. W.; Vermeulen, N. A.; Wang, T. C.; Hupp, J. T.; Farha, O. K. Best Practices for the Synthesis, Activation, and Characterization of Metal−Organic Frameworks. *Chem. Mater.* **2017**, *29*, 26−39.

(5) Silva, P.; Vilela, S. M. F.; Tomé, J. P. C.; Paz, F. A. A. Multifunctional Metal-Organic Frameworks: From Academia to Industrial Applications. *Chem. Soc. Rev.* **2015**, *44*, 6774−6803.

(6) Zhu, L.; Liu, X.-Q.; Jiang, H.-L.; Sun, L.-B. Metal-Organic Frameworks for Heterogeneous Basic Catalysis. *Chem. Rev.* **2017**, *117*, 8129−8176.

(7) Dias, E. M.; Petit, C. Towards the Use of Metal-Organic Frameworks for Water Reuse: A Review of the Recent Advances in the Field of Organic Pollutants Removal and Degradation and the Next Steps in the Field. *J. Mater. Chem. A* **2015**, *3*, 22484−22506.

(8) Horcajada, P.; Gref, R.; Baati, T.; Allan, P. K.; Maurin, G.; Couvreur, P.; Férey, G.; Morris, R. E.; Serre, C. Metal-Organic Frameworks in Biomedicine. *Chem. Rev.* **2012**, *112*, 1232−1268.

(9) Wu, M.-X.; Yang, Y.-W. Metal−Organic Framework (MOF)-Based Drug/Cargo Delivery and Cancer Therapy. *Adv. Mater.* **2017**, *29*, 1606134.

(10) Wang, Z.; Cohen, S. M. Postsynthetic Modification of Metal-Organic Frameworks. *Chem. Soc. Rev.* **2009**, *38*, 1315−1329.

(11) Stock, N.; Biswas, S. Synthesis of Metal-Organic Frameworks (MOFs): Routes to Various MOF Topologies, Morphologies, and Composites. *Chem. Rev.* **2012**, *112*, 933−969.

(12) Islamoglu, T.; Goswami, S.; Li, Z.; Howarth, A. J.; Farha, O. K.; Hupp, J. T. Postsynthetic Tuning of Metal-Organic Frameworks for Targeted Applications. *Acc. Chem. Res.* **2017**, *50*, 805−813.

(13) Liu, B.; Jie, S.; Bu, Z.; Li, B.-G. Postsynthetic Modification of Mixed-Linker Metal-Organic Frameworks for Ethylene Oligomerization. *RSC Adv.* **2014**, *4*, 62343−62346.

(14) Cohen, S. M. Modifying MOFs: New Chemistry, New Materials. *Chem. Sci.* **2010**, *1*, 32−36.

(15) Tanabe, K. K.; Cohen, S. M. Postsynthetic Modification of Metal-Organic frameworks—a Progress Report. *Chem. Soc. Rev.* **2011**, *40*, 498−519.

DOI: 10.1021/acsomega.9b01139
ACS Omega 2019, 4, 9860−9867

(16) Cohen, S. M. Postsynthetic Methods for the Functionalization of Metal-Organic Frameworks. *Chem. Rev.* **2012**, *112*, 970−1000.
(17) Jiang, D.; Keenan, L. L.; Burrows, A. D.; Edler, K. J. Synthesis and Post-Synthetic Modification of MIL-101(Cr)-NH_2 *via* a Tandem Diazotisation Process. *Chem. Commun.* **2012**, *48*, 12053−12055.
(18) Marshall, R. J.; Forgan, R. S. Postsynthetic Modification of Zirconium Metal-Organic Frameworks. *Eur. J. Inorg. Chem.* **2016**, *27*, 4310−4331.
(19) Lee, Y.-R.; Yu, K.; Ravi, S.; Ahn, W.-S. Selective Adsorption of Rare Earth Elements over Functionalized Cr-MIL-101. *ACS Appl. Mater. Interfaces* **2018**, *10*, 23918−23927.
(20) Burrows, A. D.; Keenan, L. L. Conversion of Primary Amines into Secondary Amines on a Metal-Organic Framework Using a Tandem Post-Synthetic Modification. *CrystEngComm* **2012**, *14*, 4112−4114.
(21) Hintz, H.; Wuttke, S. Solvent-Free and Time Efficient Postsynthetic Modification of Amino-Tagged Metal-Organic Frameworks with Carboxylic Acid Derivatives. *Chem. Mater.* **2014**, *26*, 6722−6728.
(22) Wittmann, T.; Siegel, R.; Reimer, N.; Milius, W.; Stock, N.; Senker, J. Enhancing the Water Stability of Al-MIL-101-NH_2 via Postsynthetic Modification. *Chem. − Eur. J.* **2015**, *21*, 314−323.
(23) Zhu, J.; Wu, L.; Bu, Z.; Jie, S.; Li, B.-G. Polyethyleneimine-Modified UiO-66-NH_2(Zr) Metal−Organic Frameworks: Preparation and Enhanced CO_2 Selective Adsorption. *ACS Omega* **2019**, *4*, 3188−3197.
(24) Hintz, H.; Wuttke, S. Postsynthetic Modification of an Amino-Tagged MOF Using Peptide Coupling Reagents: A Comparative Study. *Chem. Commun.* **2014**, *50*, 11472−11475.
(25) Wang, H.; Dong, X.; Lin, J.; Teat, S. J.; Jensen, S.; Cure, J.; Alexandrov, E. V.; Xia, Q.; Tan, K.; Wang, Q.; Olson, D. H.; Proserpio, D. M.; Chabal, Y. J.; Thonhauser, T.; Sun, J.; Han, Y.; Li, J. Topologically Guided Tuning of Zr-MOF Pore Structures for Highly Selective Separation of C_6 Alkane Isomers. *Nat. Commun.* **2018**, *9*, 1745.
(26) Pankajakshan, A.; Sinha, M.; Ojha, A. A.; Mandal, S. Water-Stable Nanoscale Zirconium-Based Metal−Organic Frameworks for the Effective Removal of Glyphosate from Aqueous Media. *ACS Omega* **2018**, *3*, 7832−7839.
(27) Zhang, J.; Yao, S.; Liu, S.; Liu, B.; Sun, X.; Zheng, B.; Li, G.; Li, Y.; Huo, Q.; Liu, Y. Enhancement of Gas Sorption and Separation Performance Via Ligand Functionalization within Highly Stable Zirconium-Based Metal-Organic Frameworks. *Cryst. Growth Des.* **2017**, *17*, 2131−2139.
(28) Naeem, A.; Ting, V. P.; Hintermair, U.; Tian, M.; Telford, R.; Halim, S.; Nowell, H.; Hołyńska, M.; Teat, S. J.; Scowen, I. J.; Nayak, S. Mixed-Linker Approach in Designing Porous Zirconium-Based Metal-Organic Frameworks with High Hydrogen Storage Capacity. *Chem. Commun.* **2016**, *52*, 7826−7829.
(29) Orellana-Tavra, C.; Marshall, R. J.; Baxter, E. F.; Lázaro, I. A.; Tao, A.; Cheetham, A. K.; Forgan, R. S.; Fairen-Jimenez, D. Drug Delivery and Controlled Release from Biocompatible Metal-Organic Frameworks Using Mechanical Amorphization. *J. Mater. Chem. B* **2016**, *4*, 7697−7707.
(30) Mocniak, K. A.; Kubajewska, I.; Spillane, D. E. M.; Williams, G. R.; Morris, R. E. Incorporation of Cisplatin into the Metal−organic Frameworks UiO66-NH_2 and UiO66-Encapsulation *vs.* Conjugation. *RSC Adv.* **2015**, *5*, 83648−83656.
(31) Sánchez-Sánchez, Á.; Suárez-García, F.; Martínez-Alonso, A.; Tascón, J. M. D. pH-Responsive Ordered Mesoporous Carbons for Controlled Ibuprofen Release. *Carbon* **2015**, *94*, 152−159.
(32) Mazaleuskaya, L. L.; Theken, K. N.; Gong, L.; Thorn, C. F.; Fitzgerald, G. A.; Altman, R. B.; Klein, T. E. PharmGKB Summary: Ibuprofen Pathways. *Pharmacogenet. Genomics* **2015**, *25*, 96−106.
(33) Yang, P.; Gai, S.; Lin, J. Functionalized Mesoporous Silica Materials for Controlled Drug Delivery. *Chem. Soc. Rev.* **2012**, *41*, 3679−3698.
(34) Ladrón de Guevara-Fernández, S.; Ragel, C. V.; Vallet-Regı, M. Bioactive Glass-Polymer Materials for Controlled Release of Ibuprofen. *Biomaterials* **2003**, *24*, 4037−4043.
(35) Das, S.; Subuddhi, U. Controlled Delivery of Ibuprofen from Poly(Vinyl Alcohol)-Poly(Ethylene Glycol) Interpenetrating Polymeric Network Hydrogels. *J. Pharm. Anal.* **2019**, *9*, 108−116.
(36) Wang, Z.; Xie, C.; Luo, F.; Li, P.; Xiao, X. P25 Nanoparticles Decorated on Titania Nanotubes Arrays as Effective Drug Delivery System for Ibuprofen. *Appl. Surf. Sci.* **2015**, *324*, 621−626.
(37) Dziadkowiec, J.; Mansa, R.; Quintela, A.; Rocha, F.; Detellier, C. Preparation, Characterization and Application in Controlled Release of Ibuprofen-Loaded Guar Gum/Montmorillonite Bionanocomposites. *Appl. Clay Sci.* **2017**, *135*, 52−63.
(38) Horcajada, P.; Serre, C.; Vallet-Regí, M.; Sebban, M.; Taulelle, F.; Férey, G. Metal-Organic Frameworks as Efficient Materials for Drug Delivery. *Angew. Chem., Int. Ed.* **2006**, *45*, 5974−5978.
(39) Rojas, S.; Colinet, I.; Cunha, D.; Hidalgo, T.; Salles, F.; Serre, C.; Guillou, N.; Horcajada, P. Toward Understanding Drug Incorporation and Delivery from Biocompatible Metal−Organic Frameworks in View of Cutaneous Administration. *ACS Omega* **2018**, *3*, 2994−3003.
(40) Xie, Y.; Liu, X.; Ma, X.; Duan, Y.; Yao, Y.; Cai, Q. Small Titanium-Based MOFs Prepared with the Introduction of Tetraethyl Orthosilicate and their Potential for Use in Drug Delivery. *ACS Appl. Mater. Interfaces* **2018**, *10*, 13325−13332.
(41) Wu, Y. N.; Zhou, M.; Li, S.; Li, Z.; Li, J.; Wu, B.; Li, G.; Li, F.; Guan, X. Magnetic Metal-Organic Frameworks: γ-Fe_2O_3@MOFs Via Confined In Situ Pyrolysis Method for Drug Delivery. *Small* **2014**, *10*, 2927−2936.
(42) Motakef-Kazemi, N.; Shojaosadati, S. A.; Morsali, A. *In Situ* Synthesis of a Drug-Loaded MOF at Room Temperature. *Microporous Mesoporous Mater.* **2014**, *186*, 73−79.
(43) Hu, Q.; Yu, J.; Liu, M.; Liu, A.; Dou, Z.; Yang, Y. A Low Cytotoxic Cationic Metal−Organic Framework Carrier for Controllable Drug Release. *J. Med. Chem.* **2014**, *57*, 5679−5685.
(44) Levine, D. J.; Runčevski, T.; Kapelewski, M. T.; Keitz, B. K.; Oktawiec, J.; Reed, D. A.; Mason, J. A.; Jiang, H. Z. H.; Colwell, K. A.; Legendre, C. M.; FitzGerald, S. A.; Long, J. R. Olsalazine-Based Metal-Organic Frameworks as Biocompatible Platforms for H_2 Adsorption and Drug Delivery. *J. Am. Chem. Soc.* **2016**, *138*, 10143−10150.
(45) Min, K. H.; Park, K.; Kim, Y.-S.; Bae, S. M.; Lee, S.; Jo, H. G.; Park, R.-W.; Kim, I.-S.; Jeong, S. Y.; Kim, K.; Kwon, I. C. Hydrophobically Modified Glycol Chitosan Nanoparticles-Encapsulated Camptothecin Enhance the Drug Stability and Tumor Targeting in Cancer Therapy. *J. Controlled Release* **2008**, *127*, 208−218.
(46) Wang, J. J.; Zeng, Z. W.; Xiao, R. Z.; Xie, T.; Zhou, G. L.; Zhan, X. R.; Wang, S. L. Recent Advances of Chitosan Nanoparticles as Drug Carriers. *Int. J. Nanomed.* **2011**, *6*, 765−774.
(47) Li, J.; Shen, S.; Kong, F.; Jiang, T.; Tang, C.; Yin, C. Effects of Pore Size on *in vitro* and *in vivo* anticancer Efficacies of Mesoporous Silica Nanoparticles. *RSC Adv.* **2018**, *8*, 24633−24640.
(48) McKinlay, A. C.; Morris, R. E.; Horcajada, P.; Férey, G.; Gref, R.; Couvreur, P.; Serre, C. BioMOFs: Metal-Organic Frameworks for Biological and Medical Applications. *Angew. Chem., Int. Ed.* **2010**, *49*, 6260−6266.
(49) Zhou, F.; Zhou, J.; Gao, X.; Kong, C.; Chen, L. Facile Synthesis of MOFs with Uncoordinated Carboxyl Groups for Selective CO_2 Capture *via* Postsynthetic Covalent Modification. *RSC Adv.* **2017**, *7*, 3713−3719.
(50) Sarker, M.; Song, J. Y.; Jhung, S. H. Carboxylic-Acid-Functionalized UiO-66-NH_2: A Promising Adsorbent for both Aqueous- and Non-Aqueous-Phase Adsorptions. *Chem. Eng. J.* **2018**, *331*, 124−131.
(51) Ahmed, I.; Khan, N. A.; Jhung, S. H. Adsorptive Denitrogenation of Model Fuel by Functionalized UiO-66 with Acidic and Basic Moieties. *Chem. Eng. J.* **2017**, *321*, 40−47.
(52) Song, J. Y.; Ahmed, I.; Seo, P. W.; Jhung, S. H. UiO-66-Type Metal-Organic Framework with Free Carboxylic Acid: Versatile

DOI: 10.1021/acsomega.9b01139
ACS Omega 2019, 4, 9860−9867

Adsorbents Via H-Bond for both Aqueous and Nonaqueous Phases. *ACS Appl. Mater. Interfaces* **2016**, *8*, 27394−27402.
(53) Sarker, M.; An, H. J.; Jhung, S. H. Adsorptive Removal of Indole and Quinoline from Model Fuel over Various UiO-66s: Quantitative Contributions of H-Bonding and Acid-Base Interactions to Adsorption. *J. Phys. Chem. C* **2018**, *122*, 4532−4539.
(54) Lin, K.-Y. A.; Lee, W.-D. Self-Assembled Magnetic Graphene Supported ZIF-67 as a Recoverable and Efficient Adsorbent for Benzotriazole. *Chem. Eng. J.* **2016**, *284*, 1017−1027.
(55) Wang, T.; Zhao, P.; Zhao, Q.; Wang, B.; Wang, S. The Mechanism for Increasing the Oral Bioavailability of Poorly Water-Soluble Drugs Using Uniform Mesoporous Carbon Spheres as a Carrier. *Drug Delivery* **2016**, *23*, 420−428.
(56) Hasan, Z.; Jhung, S. H. Removal of Hazardous Organics from Water Using Metal-Organic Frameworks (MOFs): Plausible Mechanisms for Selective Adsorptions. *J. Hazard. Mater.* **2015**, *283*, 329−339.
(57) Ahmed, I.; Jhung, S. H. Applications of Metal-Organic Frameworks in Adsorption/Separation Processes Via Hydrogen Bonding Interactions. *Chem. Eng. J.* **2017**, *310*, 197−215.
(58) Sarker, M.; Shin, S.; Jhung, S. H. Functionalized Mesoporous Metal-Organic Framework PCN-100: An Efficient Carrier for Vitamin E Storage and Delivery. *J. Ind. Eng. Chem.* **2019**, *74*, 158−163.
(59) Sarker, M.; Song, J. Y.; Jhung, S. H. Adsorptive Removal of Anti-Inflammatory Drugs from Water Using Graphene Oxide/Metal-Organic Framework Composites. *Chem. Eng. J.* **2018**, *335*, 74−81.
(60) Sarker, M.; Shin, S.; Jeong, J. H.; Jhung, S. H. Mesoporous Metal-Organic Framework PCN-222(Fe): Promising Adsorbent for Removal of Big Anionic and Cationic Dyes from Water. *Chem. Eng. J.* **2019**, *371*, 252−259.
(61) Ahmed, I.; Khan, N. A.; Jhung, S. H. Graphite Oxide/Metal-Organic Framework (MIL-101): Remarkable Performance in the Adsorptive Denitrogenation of Model Fuels. *Inorg. Chem.* **2013**, *52*, 14155−14161.
(62) Huang, X.; Brazel, C. S. On the Importance and Mechanisms of Burst Release in Matrix-Controlled Drug Delivery Systems. *J. Controlled Release* **2001**, *73*, 121−136.
(63) Da Silva, E. P.; Guilherme, M. R.; Garcia, F. P.; Nakamura, C. V.; Cardozo-Filho, L.; Alonso, C. G.; Rubira, A. F.; Kunita, M. H. Drug Release Profile and Reduction in the In Vitro Burst Release from Pectin/HEMA Hydrogel Nanocomposites Crosslinked with Titania. *RSC Adv.* **2016**, *6*, 19060−19068.
(64) Nguyen, M. H.; Tran, T. T.; Hadinoto, K. Controlling the Burst Release of Amorphous Drug-Polysaccharide Nanoparticle Complex Via Crosslinking of the Polysaccharide Chains. *Eur. J. Pharm. Biopharm.* **2016**, *104*, 156−163.
(65) Horcajada, P.; Chalati, T.; Serre, C.; Gillet, B.; Sebrie, C.; Baati, T.; Eubank, J. F.; Heurtaux, D.; Clayette, P.; Kreuz, C.; Chang, J.-S.; Hwang, Y. K.; Marsaud, V.; Bories, P.-N.; Cynober, L.; Gil, S.; Férey, G.; Couvreur, P.; Gref, R. Porous Metal-Organic-Framework Nanoscale Carriers as a Potential Platform for Drug delivery and Imaging. *Nat. Mater.* **2010**, *9*, 172−178.
(66) Hasan, Z.; Khan, N. A.; Jhung, S. H. Adsorptive Removal of Diclofenac Sodium from Water with Zr-Based Metal−Organic Frameworks. *Chem. Eng. J.* **2016**, *284*, 1406−1413.
(67) Horcajada, P.; Serre, C.; Maurin, G.; Ramsahye, N. A.; Balas, F.; Vallet-Regí, M.; Sebban, M.; Taulelle, F.; Férey, G. Flexible Porous Metal-Organic Frameworks for a Controlled Drug Delivery. *J. Am. Chem. Soc.* **2008**, *130*, 6774−6780.
(68) Xu, W.; Gao, Q.; Xu, Y.; Wu, D.; Sun, Y.; Shen, W.; Deng, F. Controllable Release of Ibuprofen from Size-Adjustable and Surface Hydrophobic Mesoporous Silica Spheres. *Powder Technol.* **2009**, *191*, 13−20.
(69) Bhadra, B. N.; Ahmed, I.; Kim, S.; Jhung, S. H. Adsorptive Removal of Ibuprofen and Diclofenac from Water Using Metal-Organic Framework-Derived Porous Carbon. *Chem. Eng. J.* **2017**, *314*, 50−58.
(70) Bůek, D.; Demel, J.; Lang, K. Zirconium Metal−Organic Framework UiO-66: Stability in an Aqueous Environment and its Relevance for Organophosphate Degradation. *Inorg. Chem.* **2018**, *57*, 14290−14297.

DOI: 10.1021/acsomega.9b01139
ACS Omega 2019, 4, 9860−9867